Pump-probe photodepletion spectroscopy of $(C_6H_6)_2^+$. Identification of spectrum in the charge resonance band region

Kazuhiko Ohashi [a], **Yoshiya Inokuchi** [a,b], **Nobuyuki Nishi** [a,b]

[a]*Institute for Molecular Science, Myodaiji, Okazaki 444, Japan*
[b]*Department of Chemistry, Faculty of Science, Kyushu University,*
Hakozaki, Fukuoka 812-81, Japan

Abstract

Pump-probe photodepletion (hole-burning) experiments are performed on mass-selected cluster ions in the gas phase. An electronic spectrum of $(C_6H_6)_2^+$ in near-infrared region comprises two charge resonance bands at 920 and 1160 nm. Intensities of these two bands monitored by the probe laser are shown to be reduced by the same amount with the introduction of the pump laser. The behavior proves that the CR bands are due to two distinct transitions of a single isomer. No evidence is found for the existence of other isomers of $(C_6H_6)_2^+$.

1. Introduction

Photodissociation spectroscopy of mass-selected cluster ions is one of the most useful technique in cluster ion spectroscopy [1,2]. The spectroscopy utilizes the dissociation process as a means to detect photoabsorption. A first mass filter isolates cluster ions of a specific size. Photoexcitation of the ions by a laser results in the dissociation. Then a second mass spectrometer detects the resultant fragment ions. The method has the advantage that, through mass selection prior to the photoexcitation, different sizes of cluster ions can be distinguished and investigated separately. Cluster ions of a given size, however, can exist in several isomeric forms. Different isomers with the same mass cannot be distinguished by such a method. For neutral clusters, several groups have successfully applied optical pump-probe depletion techniques, based on a concept similar to solid-state spectral hole-burning, to distinguish different isomers formed in a supersonic jet [3]. The principle of the spectral hole-burning in the jet was given by Lipert and Colson [4,5] and Wittmeyer and Topp [6]. Shortly, the probe laser is fixed at a wavelength resonant with an electronic transition of an isomer. The signal intensity generated by the probe laser is proportional to the ground state population of the isomer. The hole-burning laser, preceding the probe laser in time, depopulates the ground state of the isomer selected by the probe laser. The depopulation is seen as a depletion (a hole) of the signal monitored by the probe laser. Here we demonstrate that the similar idea can be applied to the photodissociation spectroscopy of mass-selected cluster ions.

We measured the photodissociation spectrum of $(C_6H_6)_2^+$ in the wavelength range of 400–1400 nm [7–9]. The spectrum exhibits two charge resonance (CR) bands at 920 and 1160 nm. One may suppose that conformational isomers of $(C_6H_6)_2^+$ are responsible for the appearance of the two CR bands. According to *ab initio* molecular orbital (MO) calculations, both T-shape and parallel isomers were found to be located at the potential-energy minima [10]. Alternatively, we have shown that two distinct transitions are possible in a single isomer [9], when it has a displaced sandwich structure with symmetry lower than D_{6h} [11]. The main purpose of the present study is to address the issue of the isomers of $(C_6H_6)_2^+$.

2. Experimental

The hole-burning experiment on mass-selected $(C_6H_6)_2^+$ is carried out by using a cluster beam apparatus with a reflectron-type time-of-flight mass spectrometer [7]. Figure 1 schematically illustrates the layout of ion production through detection. Neutral clusters are formed in a pulsed supersonic expansion. After passing through a skimmer and a collimator, the cluster beam enters an acceleration region of the mass spectrometer. Here a pulsed ionization laser ($\lambda_i = 210$ nm) intersects the cluster beam; the neutral clusters of all sizes are non-selectively ionized by 2-photon absorption via the S_2 state [9]. The 2-photon ionization at 210 nm leads to large excess energy, producing hot cluster ions. However, they loose large parts of the internal energies instantaneously by evaporating neutral molecules in the focus of the ionization laser [12]. Most of $(C_6H_6)_2^+$ ions under the following investigation originate from larger clusters through evaporative cooling processes, although the initial sizes of the clusters cannot be specified here. While traveling in the acceleration region, the packet of $(C_6H_6)_2^+$ is irradiated by a pulsed hole-burning laser ($\lambda_h = 920$ nm). Excitation by the laser leads to dissociation of $(C_6H_6)_2^+$ into $C_6H_6^+$ and C_6H_6, yielding a permanent reduction of the number of the $(C_6H_6)_2^+$ ions in the packet. The packet of the remaining $(C_6H_6)_2^+$ ions is separated from that of the product $C_6H_6^+$ during the secondary acceleration. Both ion packets are then introduced into a field-free drift region of the mass spectrometer. Here the packet of $(C_6H_6)_2^+$ is crossed by a pulsed probe laser ($\lambda_p = 850$–1210 nm). In order to change the probe wavelength quickly between 850 and 1210 nm, we use the idler output from an optical parametric oscillator (Spectra-Physics MOPO-730) pumped with a Nd:YAG laser (Spectra-Physics GCR-250). Excitation by the probe laser also leads to dissociation of $(C_6H_6)_2^+$, producing $C_6H_6^+$ and C_6H_6. Finally, the packets of the fragment ions are reflected by a two-stage ion reflector and detected by a dual microchannel plate detector.

In this experiment, both the pump and the probe laser generate the same fragment ion. A key to the experiment is to detect the fragment ion generated by each laser separately. Owing to the secondary acceleration, the packet of $C_6H_6^+$ generated by λ_h (○) arrives at the detector earlier than that of $C_6H_6^+$ produced by λ_p (●). Thus we can distinguish the $C_6H_6^+$ signal due to λ_h from the signal due to λ_p in an arrival-time spectrum.

3. Results and discussion

3.1. Photodissociation spectrum of $(C_6H_6)_2^+$ in the charge resonance band region

Figure 2 shows the photodissociation spectrum of $(C_6H_6)_2^+$ in the 700–1400 nm region. The band centered at 920 nm is assigned to a CR band of $(C_6H_6)_2^+$ [8,9]. The structureless shape of the band is predicted from a pseudo-homonuclear diatomic model for homomolecular dimer ions [13]. When $C_6H_6^+$ and C_6H_6 are located together, charge exchange between the two benzene molecules leads to the splitting into the two states: the lower bound state and the higher repulsive state. Since the CR band is due to a transition from the bound state to the repulsive state, the band is inherently structureless. According to "reflection" model [14], the width of the band is interpreted to be given by reflecting the square of the vibrational eigenfunction in the ground state at the upper repulsive potential curve.

The spectrum of $(C_6H_6)_2^+$ exhibits another band centered at 1160 nm. This band is shifted by 240 nm ($\approx$2200 cm^{-1}) to the red of the 920-nm band. The intensity of this band is approximately 10 % of the 920-nm band. The corresponding band was not observed by the measurement of the absorption spectra in glassy solutions [15,16] nor in low temperature matrices [17,18]. This band is assigned to another CR band of $(C_6H_6)_2^+$ [19]. We perform the pump-probe experiment to identify the 1160-nm band.

3.2. Pump-probe photodepletion experiment

Figure 3 exhibits arrival-time spectra of the fragment ions recorded in the course of the pump-probe photodepletion experiment on $(C_6H_6)_2^+$. The top two spectra are obtained by employing the same wavelength (920 nm) for the hole-burning and the probe lasers. Only the ion signal due to the probe laser, namely the probe-laser signal, appears at 34.9 μs on spectrum (a) recorded with the probe laser alone. Introduction of the hole-burning laser yields spectrum (b). Since both lasers are tuned in to 920 nm to dissociate the same isomer, a hole is certainly produced in the probe-laser signal. Spectrum (b) actually shows a decrease in the probe-laser signal with respect to the corresponding signal on spectrum (a). Because of the secondary acceleration, the ion signal due to the hole-burning laser shifts to a shorter time and appears at

30.8 μs. For obtaining the bottom two spectra, the wavelength of the probe laser is changed to 1160 nm while that of the hole-burning laser is kept at 920 nm. Spectrum (c) is recorded with the probe laser alone. As can be seen on spectrum (d), the intensity of the probe-laser signal is reduced by the introduction of the hole-burning laser. The result indicates that both lasers excite the same isomer, otherwise the intensity of the probe-laser signal would have no connection with the hole-burning laser. One may suppose that the intensity of the probe-laser signal on spectrum (d) decreases because the probe laser at 1160 nm is resonant not only with the 1160-nm band but also with the tail of the 920-nm band (see the decomposed spectra shown in Fig. 2). In order to rule out this possibility, we measure the magnitude of the signal depletion,

$$\delta_{\mathrm{frag}} = [I_{\mathrm{p}}(\mathrm{off}) - I_{\mathrm{p}}(\mathrm{on})] \,/\, I_{\mathrm{p}}(\mathrm{off}), \tag{1}$$

where $I_{\mathrm{p}}(\mathrm{on})$ and $I_{\mathrm{p}}(\mathrm{off})$ indicate the intensities of the probe-laser signal taken with the hole-burning laser on and off, respectively. The value of δ_{frag} is calculated to be 0.69 from a pair of spectra (a) and (b). Spectrum (d) is recorded with approximately the same intensity of the hole-burning laser with spectrum (b). The value of δ_{frag} is 0.71 for a pair of spectra (c) and (d), which is comparable to the value from a pair of spectra (a) and (b). If the tail of the 920-nm band alone were responsible for the depletion in the intensity of the probe-laser signal on spectrum (d), the δ_{frag} value should be less than 10 % of the value from a pair of spectra (a) and (b).

The magnitude of δ_{frag} is also measured by fixing the wavelength of the hole-burning laser at 920 nm and changing the wavelength of the probe laser from 850 to 1210 nm. The intensity of the hole-burning laser is kept at a constant value in a series of the measurement. In Fig. 4, the values of δ_{frag} are plotted against the wavelength of the probe laser. At all wavelengths studied, the intensities of the probe-laser signals are reduced by 55–60 % when the hole-burning laser is introduced. This finding rules out the possibility that the two CR bands are due to two isomers of $(C_6H_6)_2^+$. If the two CR bands were due to different isomers, the value of δ_{frag} would be zero at wavelengths in the 1160-nm band region. We therefore conclude that *two distinct transitions of a single isomer* are responsible for the appearance of the two CR bands.

In addition, the value of δ_{frag} can be compared with the magnitude of the depletion in the parent ion intensity,

$$\delta_{\mathrm{dim}} = [I_{\mathrm{dim}}(\mathrm{off}) - I_{\mathrm{dim}}(\mathrm{on})] \,/\, I_{\mathrm{dim}}(\mathrm{off}), \qquad (2)$$

where $I_{\mathrm{dim}}(\mathrm{on})$ and $I_{\mathrm{dim}}(\mathrm{off})$ indicate the intensities of the parent dimer ions measured with the hole-burning laser on and off, respectively. The magnitude of the depletion is examined before and after a series of the pump-probe photodepletion measurement. During the measurement for obtaining the data plotted in Fig. 4, the values of δ_{dim} are found to be in the range of 0.57 ± 0.03, which are in agreement with the values of δ_{frag}. Figure 5 shows further comparison between δ_{frag} and δ_{dim}. Since the δ_{frag} values are independent of the probe wavelength, we average the δ_{frag} values at all wavelengths to obtain $\langle\delta_{\mathrm{frag}}\rangle$. Then $\langle\delta_{\mathrm{frag}}\rangle$ is compared with δ_{dim} measured with the same intensity of the hole-burning laser. The comparison is made at three different laser intensities. At each intensity, the two values agree with each other within the experimental uncertainties. If there were isomers of $(C_6H_6)_2^+$ that would not absorb in the near-infrared region, δ_{dim} should be smaller than δ_{frag}, because such isomers would survive the photodissociation due to the hole-burning laser. The result strongly suggests that *one single isomer of* $(C_6H_6)_2^+$ *is dominant* under our experimental conditions.

3.3. Possible structure of $(C_6H_6)_2^+$

Structure of $(C_6H_6)_2^+$ has not been determined experimentally. Based on the similarity of the absorption spectrum of $(C_6H_6)_2^+$ to that of paracyclophane cation [16], most of the condensed-phase studies suggested or supposed symmetrical sandwich structure with D_{6h} symmetry. Two benzene rings are parallel and perfectly superimposed in this structure. The MO configuration for $(C_6H_6)_2^+$ with D_{6h} symmetry is $(e_{1u})^4(e_{1g}^*)^3$, where e_{1u} (e_{1g}^*) is the bonding (antibonding) combination of the doubly degenerate highest occupied molecular orbitals of benzene (e_{1g}) [11]. Because of the degeneracy, CR bands originating from $e_{1u} \rightarrow e_{1g}^*$ transitions would be superimposed on one another.

In *ab initio* MO calculations for $(C_6H_6)_2^+$ by Yamabe *et al.*, both T-shape and parallel structures were found to be located at the potential-energy minima [10]. The T-shape structure is more stable than the parallel one according to spin-restricted open-shell Hartree-Fock MO calculations. However, they stated that the electron-correlation effect could potentially render the parallel form more favorable. Therefore, they concluded that the stabilities of the two isomers are similar to each other [10]. The conclusion is not in line with the present experimental results. We have shown that one single isomer is dominant in an ensemble of the $(C_6H_6)_2^+$ ions. Recently, we have reported that phenol dimer ion shows no strong CR band [20]. This is probably because two aromatic rings in $(C_6H_5OH)_2^+$ cannot be in a parallel configuration owing to the geometrical constraint of an O–H···O hydrogen bond. For $(C_6H_6)_2^+$, therefore, we favor parallel or approximately parallel configurations of the two aromatic rings, which allow contact of the π orbitals of the two rings. The T-shape isomer suggested by the calculations may exist but the population must be negligibly small under our experimental conditions.

Badger and Brocklehurst proposed a distorted sandwich structure for $(C_6H_6)_2^+$ [21]. By *ab initio* MO calculations for $(C_6H_6)_2^+$, Milosevich *et al*. showed that one benzene ring of each can slide for ≈ 0.04 nm to give displaced structures [11]. In the displaced structures, bonding or antibonding with respect to the intermolecular coordinate lifts the degeneracy in D_{6h} symmetry. We considered the MO configurations of $(C_6H_6)_2^+$ for the structures where one benzene ring of each is displaced along either a C_2' axis (bisector of a CCC angle) of the molecule or a C_2'' axis [9]. In either case, two transitions are shown to be allowed in C_{2h} symmetry from the group theoretical consideration. The appearance of the two CR bands can be explained by considering a displaced structure for $(C_6H_6)_2^+$. In order to discuss the structure of $(C_6H_6)_2^+$ in further detail, we have to wait for future developments in theoretical as well as experimental studies on $(C_6H_6)_2^+$.

4. Conclusion

A pump-probe technique has been presented that applies the principles of spectral hole-burning to the study of mass-selected cluster ions in the gas phase. This approach allows one to address the question of existence of a number of isomeric forms of cluster ions. The experiment has been performed on the CR bands of $(C_6H_6)_2^+$ in near-infrared wavelength region. The photodepletion behavior proves that multiple isomers are not responsible for the appearance of the two CR bands. By *ab initio* MO calculations, both T-shape and parallel structures are proposed for $(C_6H_6)_2^+$. However, the lowest-energy structure and the transition energies of the CR bands have yet to be determined by theoretical calculations of a reasonable level.

Acknowledgement

This work was supported in part by Grant-in-Aid for research programs (07740465 and 07454190) from the Ministry of Education, Science, Sports and Culture of Japan. Financial support from the Morino Science Foundation to K. O. is gratefully acknowledged.

References

[1] Ion and Cluster Ion Spectroscopy and Structure, ed. J. P. Maier (Elsevier, Amsterdam, 1989).

[2] J. M. Farrar, in: Cluster Ions, eds. C. Y. Ng, T. Baer and I. Powis (John Wiley & Sons, Chichester, 1993), p. 243.

[3] For example, W. Scherzer, H. L. Selzle and E. W. Schlag, Chem. Phys. Letters 195 (1992) 11, and references cited therein.

[4] R. J. Lipert and S. D. Colson, J. Phys. Chem. 93 (1989) 3894.

[5] R. J. Lipert and S. D. Colson, Chem. Phys. Letters 161 (1989) 303.

[6] S. A. Wittmeyer and M. R. Topp, Chem. Phys. Letters 163 (1989) 261.

[7] K. Ohashi and N. Nishi, J. Chem. Phys. 95 (1991) 4002.

[8] K. Ohashi and N. Nishi, J. Phys. Chem. 96 (1992) 2931.

[9] K. Ohashi, Y. Nakai, T. Shibata and N. Nishi, Laser Chem. 14 (1994) 3.

[10] K. Hiraoka, S. Fujimaki, K. Aruga and S. Yamabe, J. Chem. Phys. 95 (1991) 8413.

[11] S. A. Milosevich, K. Saichek, L. Hinchey, W. B. England and P. Kovacic, J. Am. Chem. Soc. 105 (1983) 1088.

[12] K. Ohashi, K. Adachi, and N. Nishi, Bull. Chem. Soc. Jpn. 69 (1996) 915.

[13] G. P. Smith and L. C. Lee, J. Chem. Phys. 69 (1978) 5393.

[14] G. Herzberg, Molecular Spectra and Molecular Structure, I. Spectra of Diatomic Molecules (Van Nostrand, New York, 1950) p. 391.

[15] T. Shida and W. H. Hamill, J. Chem. Phys. 44 (1966) 4372.

[16] B. Badger and B. Broklehurst, Trans. Faraday Soc. 65 (1969) 2582.

[17] J. H. Miller, L. Andrews, P. A. Lund and P. N. Schatz, J. Chem. Phys. 73 (1980) 4932.

[18] T. Shida, *Electronic Absorption Spectra of Radical Ions* (Elsevier, Amsterdam, 1988), p. 12.

[19] J. Tokuhiro, K. Ohtsuka, M. Fujii, N. Mikami and M. Ito, unpublished results.

[20] K. Ohashi, Y. Inokuchi and N. Nishi, Chem. Phys. Letters 257 (1996) 137.

[21] B. Badger and B. Brocklehurst, Trans. Faraday Soc. 66 (1970) 2939.

Figure Captions

Fig. 1. Schematic illustration of the layout of ion production through detection. Hole-burning laser beam (λ_h) is introduced into the acceleration region, while probe laser beam (λ_p) is introduced into the field-free region of the mass spectrometer. Owing to the secondary acceleration, the packet of the fragment ion generated by λ_h (○) arrives at the detector earlier than that produced by λ_p (●). Thus the fragment ion signal due to λ_h can be distinguished from that due to λ_p in the arrival-time spectrum (inset).

Fig. 2. Photodissociation spectrum of $(C_6H_6)_2^+$ in the 700–1400 nm region. Both of the main band at 920 nm and the relatively weak one at 1160 nm are assigned to charge resonance bands. The spectrum is decomposed into two bands by fitting experimental points (filled circles) with two functions (dotted curves), each of them is a convolution between a Gaussian and a Lorentzian. Sum of the two functions is indicated by solid curve.

Fig. 3. Arrival-time spectra of the fragment ions ($C_6H_6^+$) produced in the course of the pump-probe photodepletion experiment on $(C_6H_6)_2^+$. Spectrum (a) is recorded with the probe laser (920 nm) alone. Spectrum (b) is recorded with the hole-burning laser (920 nm) followed by the probe laser (920 nm). A pair of spectra (c) and (d) is obtained under the same conditions with a pair of spectra (a) and (b) but at a different wavelength of the probe laser (1160 nm). An ion signal due to the hole-burning laser appears at 30.8 μs, while that due to the probe laser (probe-laser signal) at 34.9 μs.

Fig. 4. Plots of the depletion yields of the probe-laser signal (δ_{frag} as defined by Eq. 1) against the probe wavelength (λ_p). The wavelength of the hole-burning laser (λ_h) is fixed at 920 nm. The dotted curve is the photodissociation spectrum of $(C_6H_6)_2^+$ for reference.

Fig. 5. Comparison of the depletion yields of the parent ion signal (δ_{dim} as defined by Eq. 2) with those of the probe-laser signal (δ_{frag}). The values of δ_{frag} at all wavelengths studied are averaged to obtain $<\delta_{frag}>$, because they are independent of the probe wavelength. Then the $<\delta_{frag}>$ values are plotted against δ_{dim} measured with the same intensity of the hole-burning laser. Solid line indicates the relation, $<\delta_{frag}> = \delta_{dim}$.

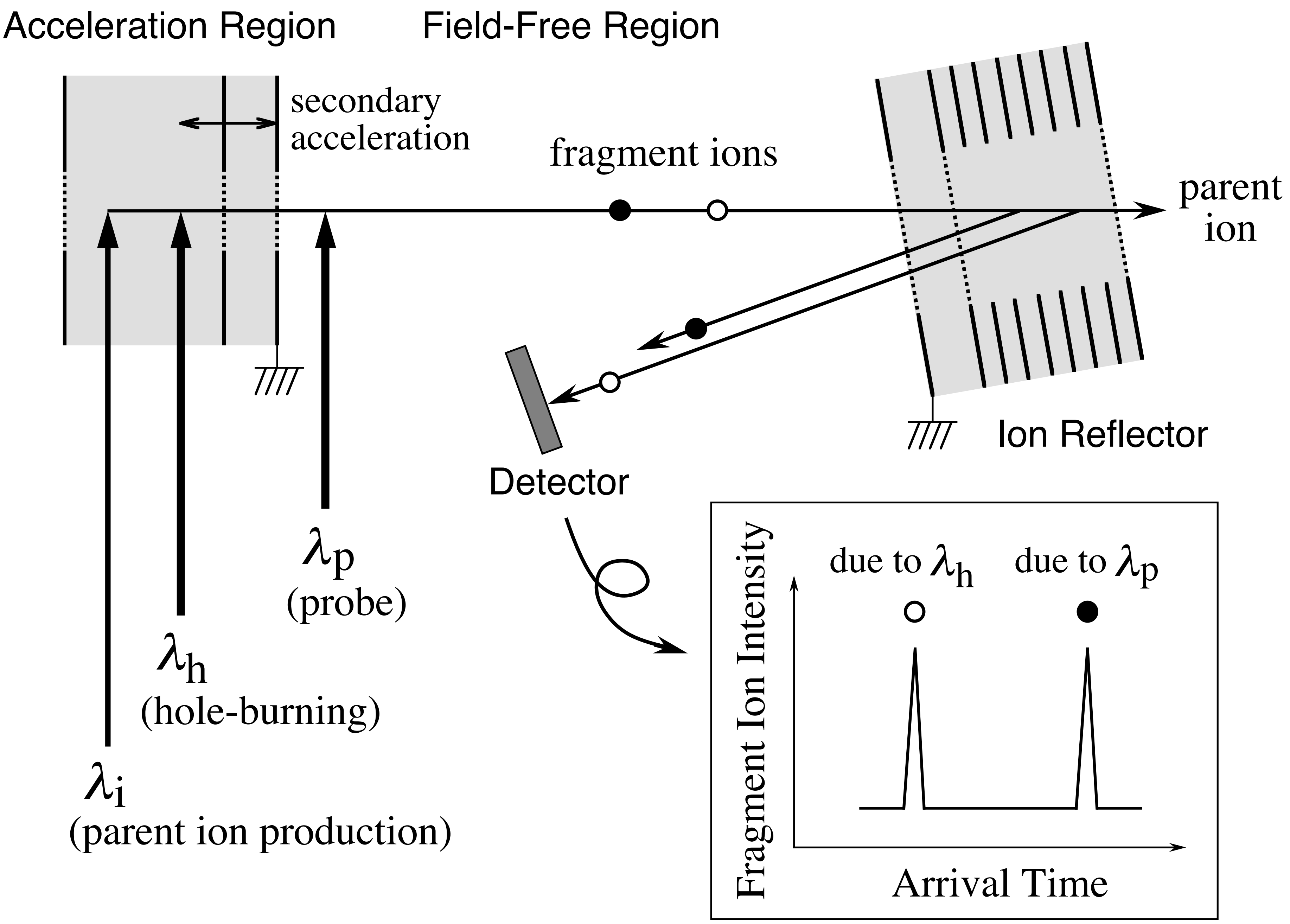

Fig. 1. Ohashi *et al.*

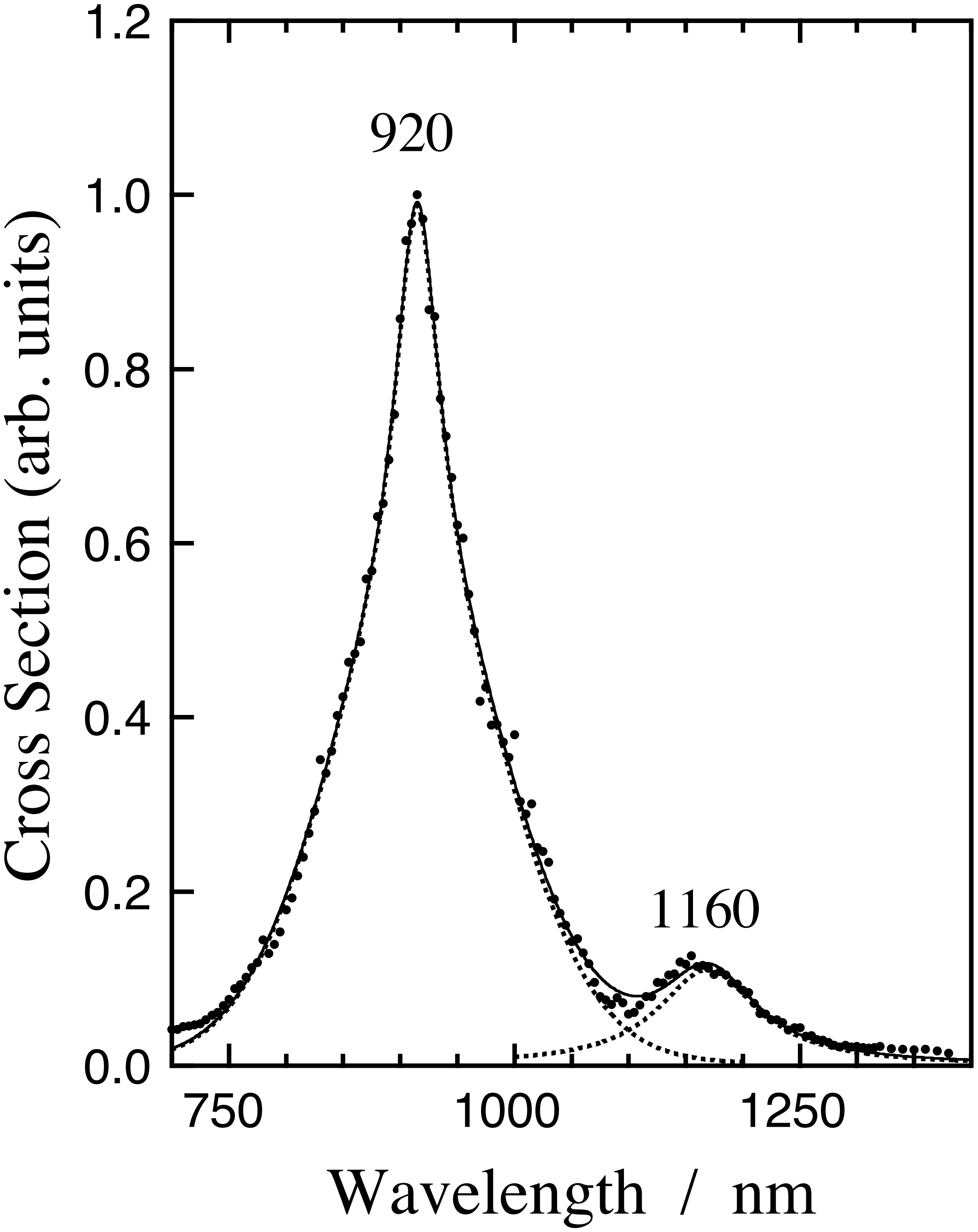

Fig. 2. Ohashi *et al*.

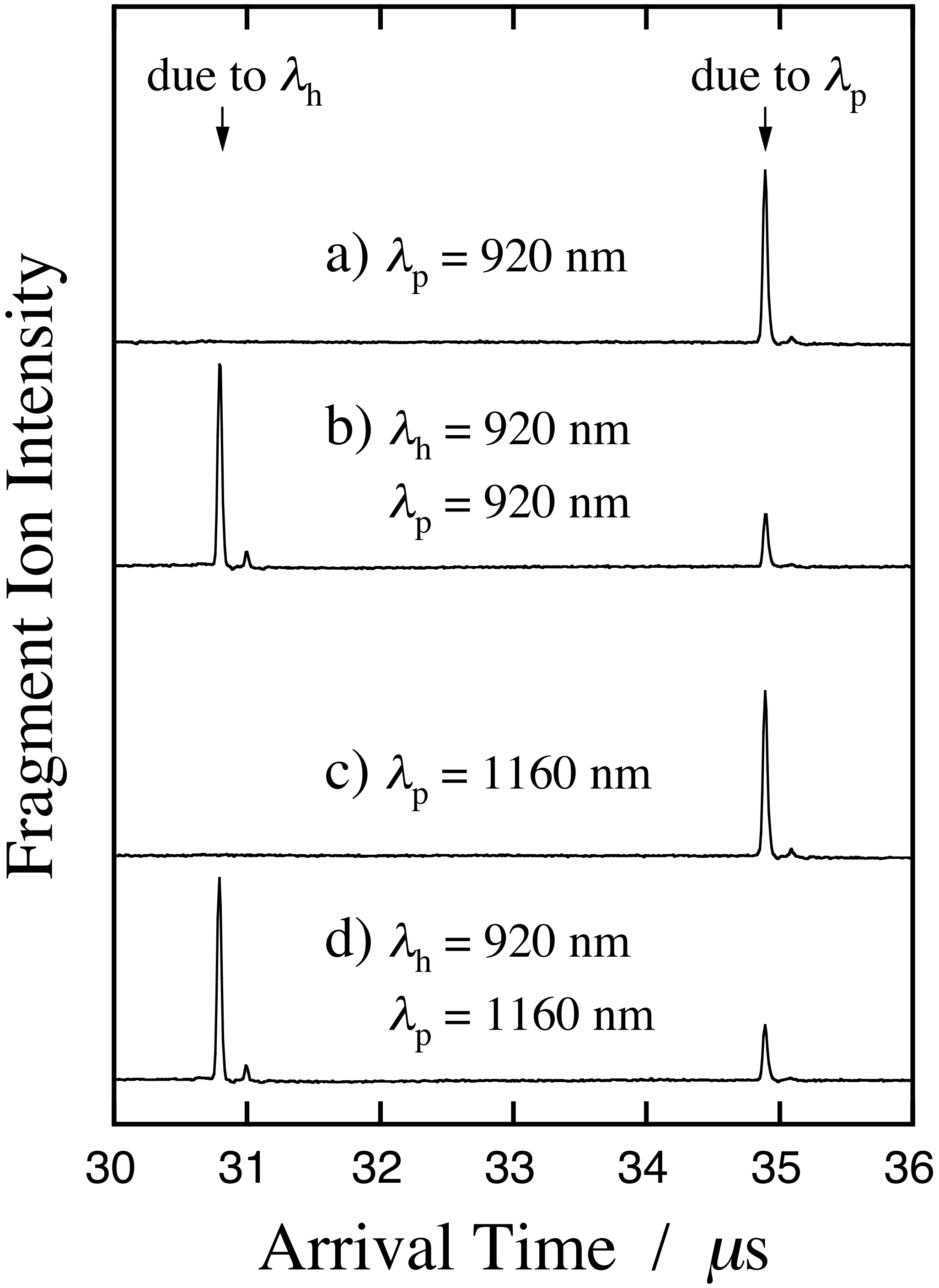

Fig. 3. Ohashi *et al*.

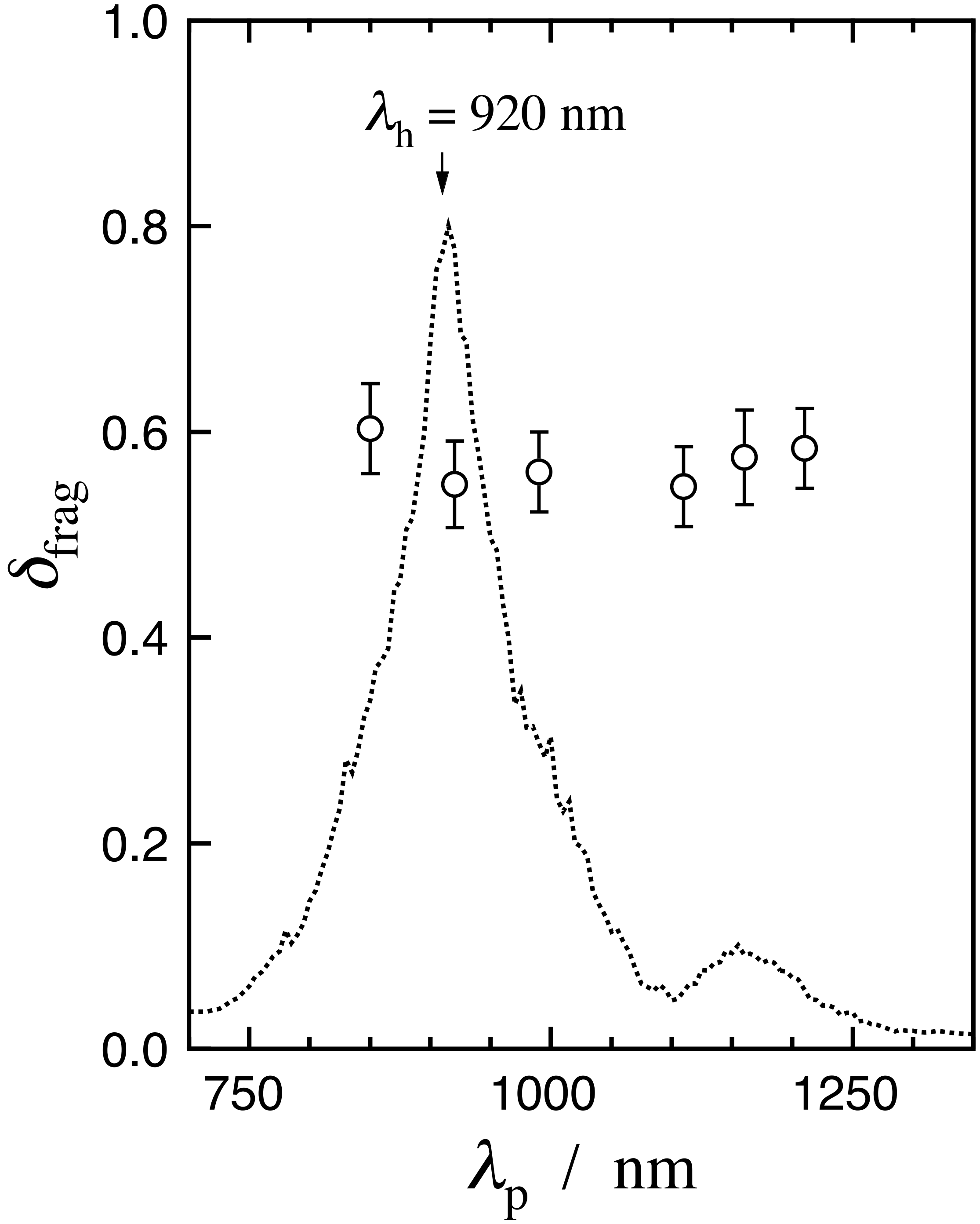

Fig. 4. Ohashi *et al*.

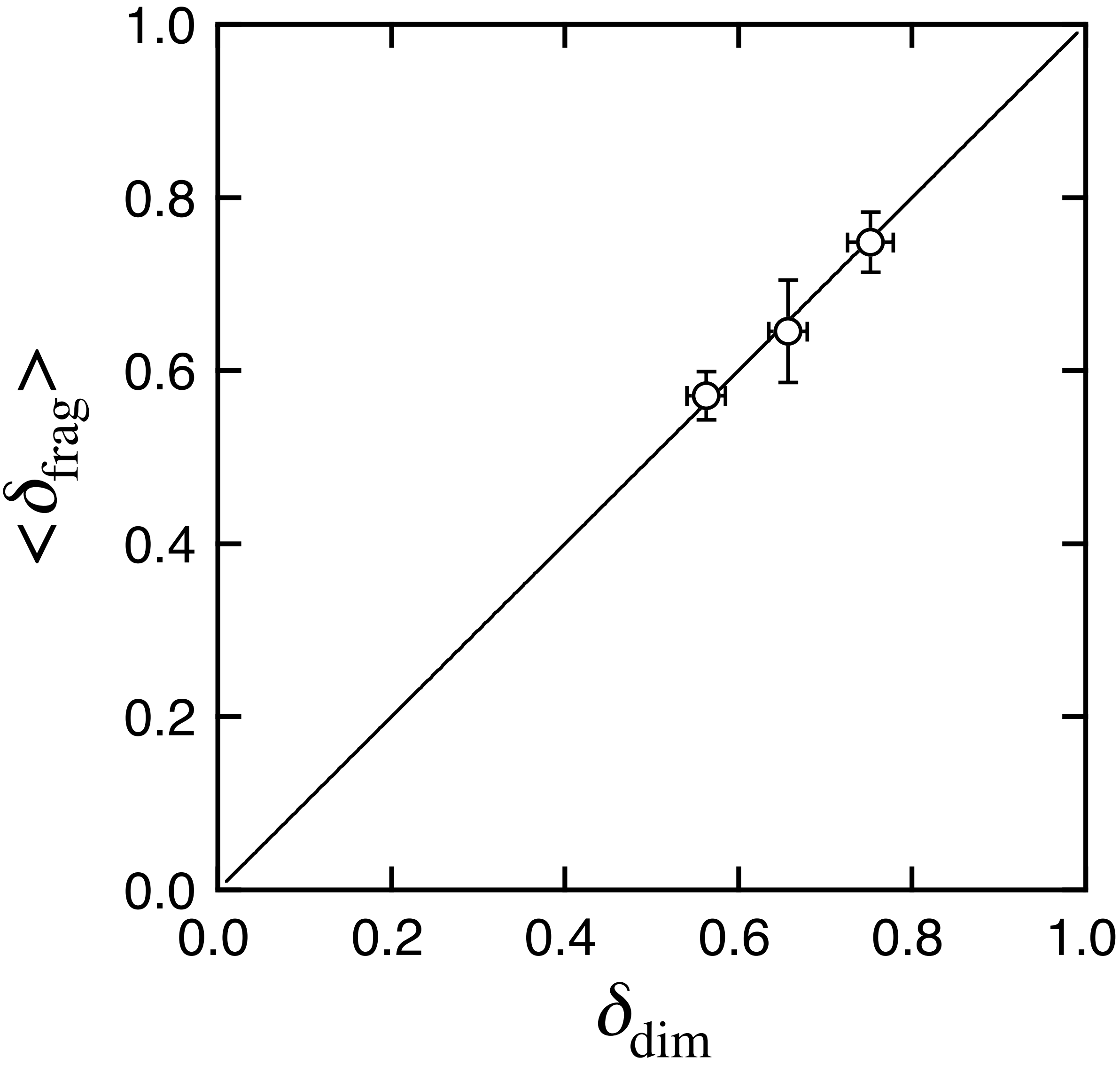

Fig. 5. Ohashi *et al*.